NATIONAL UNIVERSITY OF SCIENCE AND TECHNOLOGY

POLITEHNICA BUCHAREST

DOCTORAL SCHOOL OF MATERIALS SCIENCE AND ENGINEERING

Ph.D Thesis

Summary

Ph.D Candidate:

Eng.GHINEA ANDREI MIHAI

Ph.D Supervisor:

Prof.Em.Dr.Eng. COJOCARU MIHAI-OVIDIU

Bucharest,

2023

NATIONAL UNIVERSITY OF SCIENCE AND TECHNOLOGY

POLITEHNICA BUCHAREST

DOCTORAL SCHOOL OF MATERIALS SCIENCE AND ENGINEERING

Ph.D Thesis

STUDIES AND RESEARCH ON THE POSSIBILITIES OF CONTROL AND ACCELERATION OF THE GASEOUS NITRIDING PROCESS

Summary

Ph.D Candidate:

Eng.GHINEA ANDREI MIHAI

Ph.D Supervisor:

Prof.Em.Dr.Eng. COJOCARU MIHAI-OVIDIU

Bucharest,

2023

Keywords: nitriding, titanaliting, predictions pf phase composition, experimental program, experiment-active method, semi-empirical methods, nitrogen dilution, dissociation degree variation, nitrogen potential.

ABSTRACT

Experimental programming methods - active experiment method (methods used for process optimization) were used in each stage of the research. Thus, the effects of changing the degree of dissociation and nitrogen dilution of the atmospheres used in gaseous nitriding were studied. It has been shown analytically and experimentally that when the proportion of nitrogen in the NH_3-N_2 mixture is increased, the nitrogen potential of the atmosphere increases, the more intensely the degree of dissociation of ammonia is reduced, thus implying an amplification of the kinetics of layer growth. At the same time, thermochemical enrichment treatments with titanium and aluminium were carried out and subsequently nitrided under certain conditions (provided by the experimental programming) to follow the effect of this processing on the composition and growth kinetics of the layer. Predictions of the phasic composition of the nitrided layers upon changing the activity of the media used were made using thermodynamic calculations. Thus, the values of nitrogen potentials corresponding to the boundary limits of the different phases in the Fe-N system at equilibrium at 520 ˚C were estimated.

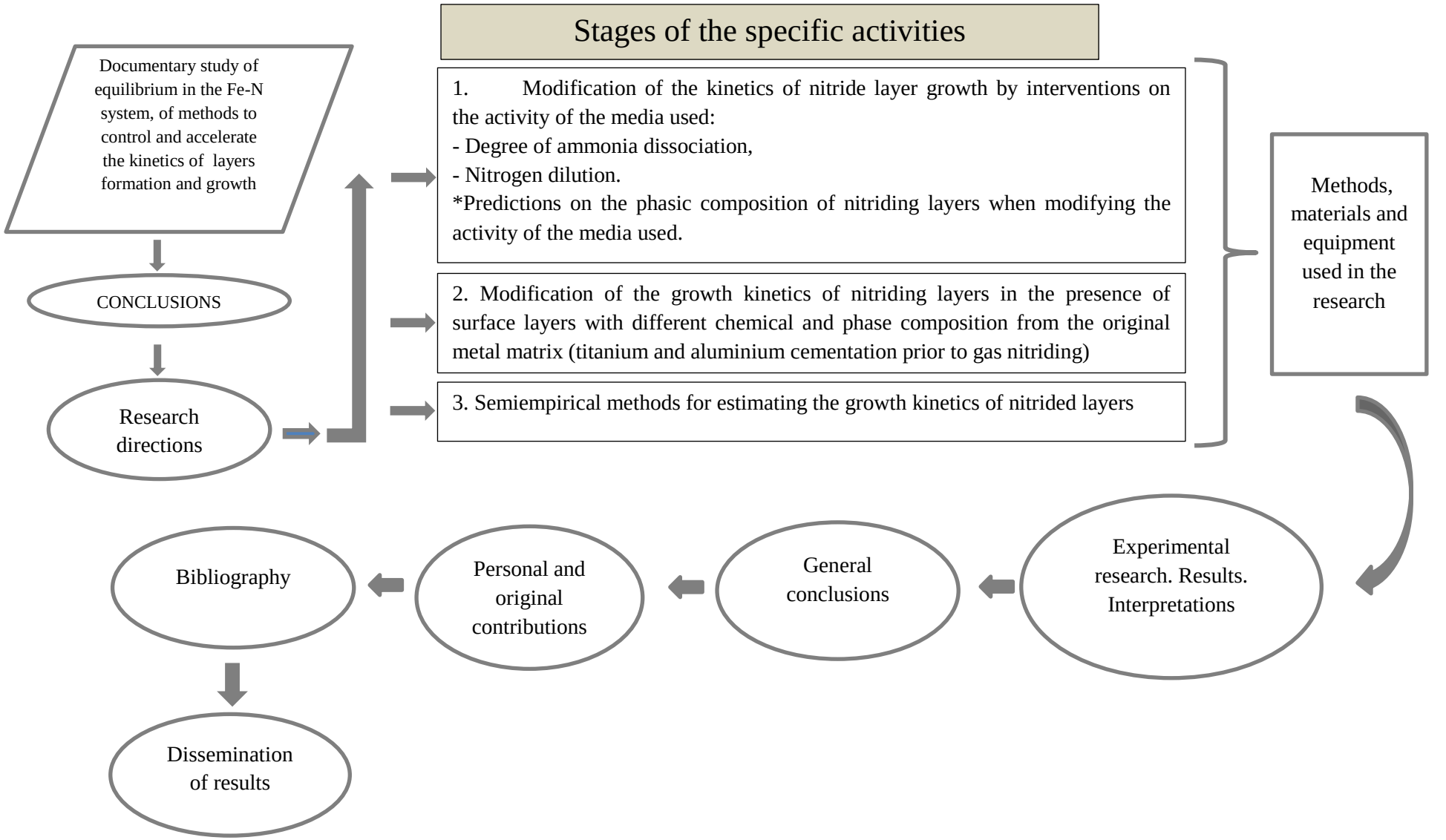
Stages of the specific activities
Documentary study of equilibrium in the Fe-N system, of methods to control and accelerate the kinetics of layers formation and growth
CONCLUSIONS
Research directions
1. Modification of the kinetics of nitride layer growth by interventions on the activity of the media used:
- Degree of ammonia dissociation,
- Nitrogen dilution.
*Predictions on the phasic composition of nitriding layers when modifying the activity of the media used.
2. Modification of the growth kinetics of nitriding layers in the presence of surface layers with different chemical and phase composition from the original metal matrix (titanium and aluminium cementation prior to gas nitriding)
3. Semiempirical methods for estimating the growth kinetics of nitrided layers
Methods, materials and equipment used in the research
Experimental research. Results. Interpretations
General conclusions
Personal and original contributions
Bibliography
Dissemination of results

CHAPTER 1

DOCUMENTARY STUDY

1.INTRODUCTION

Thermochemical treatments are thermal processes carried out in chemically controlled environments. The purpose of applying thermochemical treatments is to modify the structure and properties of the surface areas of metal products by changing their chemical and phase composition [1].

A number of researchers have made contributions to improve the Fe-N diagram and understand its transformation processes. While Paranjpe and Turkdogan studied the solubility of nitrogen in ferrite, Kester studied the aging process of nitroferrite [8-9]. Turner and Bramley investigated the range of nitrogen diffusion in austenite, and Lahtin I.M. was the first to determine nitrogen diffusion constants in different phases of the nitrided layer [10].

In order to ensure reproducibility from one batch to another, layer formation and structure must be controlled. The nitriding results depend on the process parameters (temperature, time, atmosphere used for nitriding) required to meet the specifications and the accuracy controlled during the process [4]. The mechanical properties of nitriding layers are directly related to their microstructure and the way the diffusion process has been carried out. The development of compound layers during gaseous nitriding occurs starting from the formation of the α_N solid solution followed by nucleation of the γ' nitride at the surface and nucleation of the ε phase above [16]. For the control of the nitriding atmosphere, the degree of ammonia dissociation has been adopted as a control parameter, its measurement being done by titration [17]. This measurement method is done outside the workspace, thus there is a possibility of human error. In the 1990s, a new control method based on nitrogen potential emerged, which measures the amount of hydrogen inside the plant and automatically intervenes to maintain it at a certain preset value [18].

Over the years, continuous efforts have been made to simulate the gas nitriding process, with most of the work being done to simulate the pure iron nitriding process.

The objectives of the present work, aim at highlighting certain aspects related to the kinetics of nitrided layers and the acceleration of diffusion processes, starting from the variation of the composition of gas mixtures but also of the essential parameters: degree of dissociation and temperature. In order to observe the effect it has on the growth of the layers, some thermochemical processing prior to nitridation was performed.

2. DOCUMENTARY STUDY ON THE NITRIDING PROCESS

2.1 Evolution in time of Fe-N diagram

Fe-N equilibrium diagram (Fig. 2.1, Fig. 2.2, Fig. 2.3) is one of the most widely used diagrams and has been remodelled (improved) over time. The first to create the Fe-N diagram was Fry, later Lehrer, Eisenhunt and Kaup also proposed equilibrium diagrams while retaining some elements of Fry [19]. Interest in the Fe-N diagram has not ceased since its discovery. In 1951 Jack K modified the diagram following X-ray diffraction results of iron nitrides for temperatures above 300 ˚C, later demonstrating that nitrides can also form at temperatures below this one [20]. In the 1980's due to studies carried out, the diagram was completed with data on magnetic transformations in the system (Fig. 2.2.).

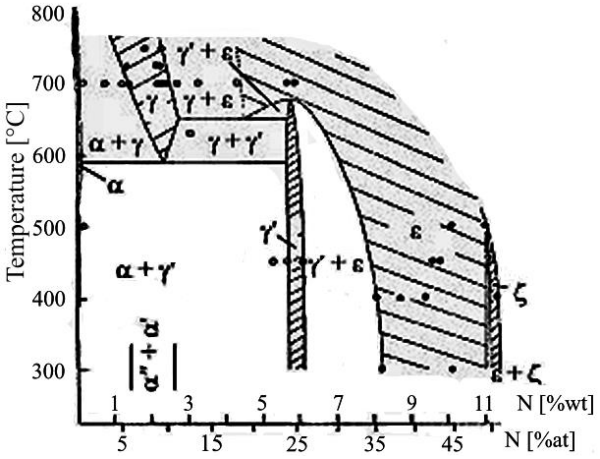

Figure 2.1. Fe-N Diagram. [21]

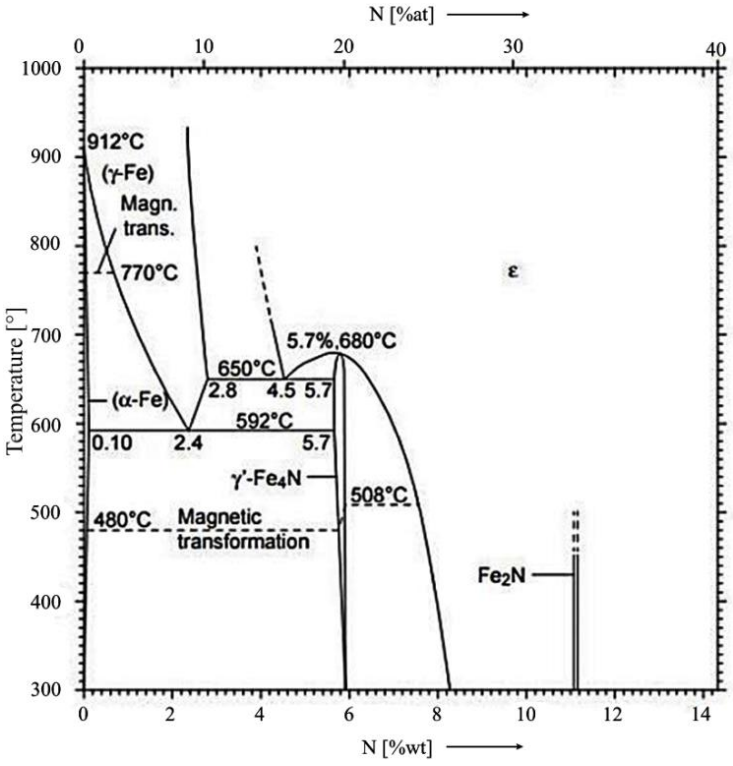

Figure 2.2. Fe-N Diagram. [25]

Analyzing the two diagrams in Fig. 2.1. and Fig. 2.2. it can be seen that the phase γ' and ζ change. The γ' phase in Fig. 2.1. has a broad concentration range at temperatures between 300 ˚C and 450 ˚C, then narrows with increasing temperature up to 680 ˚C. In Fig. 2.2., the maximum concentration range of the γ'phase is found at 650 ˚C, after which it starts to narrow up to 350˚ C, and then becomes completely stoichiometric.

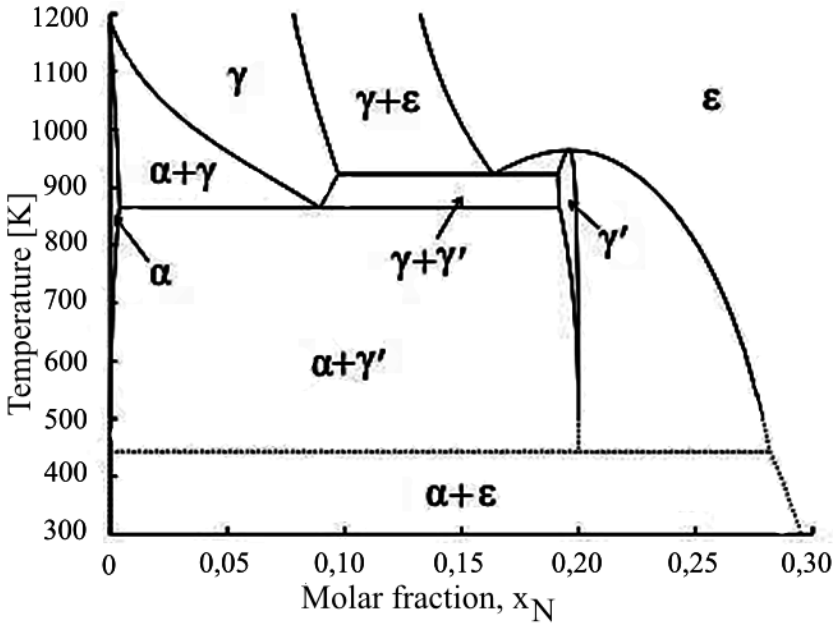

Figure 2.3. Fe-N diagram calculated using thermodynamic descriptions. [27]

There are still slightly different views in the literature on the concentration limits at which solid solutions based on compounds γ' and ε, respectively, are stable (their stoichiometry and crystallography, respectively). In this context, a particularity of the solid solution based on the defined chemical compound Fe_4N should be pointed out, namely that it is stable in an extremely narrow range of nitrogen concentrations (e.g., according to the Fe-N thermodynamic equilibrium diagram, 5.3÷5.75%N at the eutectoid transformation temperature. The literature in the field considering the Fe_4N phase, corrects the information that iron atoms are distributed in a CFC lattice with an ordered distribution of nitrogen atoms in the centers of the elementary cubes (1/2 1/2 1/2) [19]. Thus, according to Kooi, Somers, Mittemeier at.al in general solid solutions of the Fe-N system can be considered as consisting of two interleaved sublattices, one of which is assigned to iron atoms and the other to nitrogen atoms. The iron sublattice is considered to be completely occupied by iron atoms, and the nitrogen sublattice is considered to consist of octahedral interstices of the iron lattice, partially occupied by nitrogen atoms and partially by vacancies [19].

In the case of solid solutions α-Fe[N] (CVC-type iron sublattice), or γ-Fe[N] (CFC-type iron sublattice), the nitrogen atoms are more or less randomly distributed in their own sublattices, in the case of γ'-Fe_4N1-x phase (CFC-type iron sublattice), respectively ε-Fe_2N_{1-z}

(compact hexagonal-type iron sublattice) the nitrogen atoms exhibit a LONG-RANGE ORDER OF NITROGEN distribution in their own subnetworks. In the presence of alloying elements part of the iron atoms in the γ' and ε phases, respectively, is replaced by the atoms of the alloying elements thus resulting in complex nitrides of the type $(Fe,M)_4N$; $(Fe,M)_3N$; $(Fe,M)_2N$ etc. [19].

The conclusions drawn from the comparative analysis of the three equilibrium diagrams are related to the Fe_4N-γ' phase, its concentration limits and its stoichiometry. The general appearance of the diagrams remains approximately the same. The absence of Fe_4N-γ' phase below 214 ˚C does not seem justified because thermodynamically its decomposition into iron and nitrogen is not possible up to 2900 ˚C. At 2900 ˚C ΔG=-3.9 Kcal/mol and the decomposition reaction can take place.

2.2 Nitriding mechanisms

Ammonia (NH_3) is a very important component in the creation of atmospheres for thermochemical processes, and its reactions with other gases or with the surface of metals undergoing processing are of great interest. There are two main mechanisms of nitriding: mechanism of atomic adsorption and mechanism of ionic adsorption.

Grabke established in 1968 [37] and 1976 [33] that in the case of ammonia decomposition on surfaces that are non-ferrous, based on the analogy of reactions occurring on an iron surface, that the following stepwise decomposition reactions are posible:

$$NH_3(g) \leftrightarrow NH_3(ad) \quad [41] \tag{6}$$

$$NH_3(ad) \leftrightarrow NH_2(ad) + H(ad) \quad [41] \tag{7}$$

$$NH_2(ad) \leftrightarrow NH(ad) + H(ad) \quad [41] \tag{8}$$

$$NH(ad) \leftrightarrow N(ad) + H(ad) \quad [41] \tag{9}$$

$$2N(ad) \leftrightarrow N_2(ad) \quad [41] \tag{10}$$

$$N_2(ad) \leftrightarrow N_2(g) \quad [41] \tag{11}$$

$$2H(ad) \leftrightarrow H_2(g) \quad [41] \tag{12}$$

$$H_2(ad) \leftrightarrow H_2(g) \quad [41] \tag{13}$$

According to reference 47, in the reaction space during the course of gaseous nitriding, conditions exist that in the areas adjacent to the metal surfaces at the same time as the thermocatalytic dissociation of ammonia, anions or anionic complexes of ammonia are formed. This has been demonstrated theoretically and experimentally [47].

The thermocatalytic decomposition reaction of ammonia requires about 11,2 eV. In contrast the ionisation of the ammonia molecule with the formation of anions releases an energy of +2,8 eV, and the formation of cations requires 10,34 eV.

$$NH_3 + e^- = NH_3^- \quad +2{,}8eV \quad [47] \tag{17}$$

$NH_3 = NH_3^+ + e \quad -10{,}34eV$ [47] (18)

The conclusion drawn from the study of reference 47, was related to the fact that in gaseous nitridation under certain favourable conditions, non-dissociated ammonia molecules, radical, anion and cation dissociation products can exist at the same time.

2.3 Theories of layer formation

Under technical conditions the nitriding of iron and steel takes place in a partially dissociated ammonia atmosphere, the nitriding processes taking place in heterogeneous systems where the basis of the reactions are diffusion processes [50]. The nitrogen potential can be calculated according to the composition of the saturated atmosphere and the pressure ratio, thus it is possible to determine the concentration of nitrogen that can be provided in the respective atmosphere [51].

From thermodynamic calculations it is found that dilution of NH_3 with N_2 and Ar leads to the stability of the formation of ε and γ' phases and the broadening of the domains in which they are found. In the case of using H_2 as dilution the domains of ε and γ' phases decrease and the domain of α phase increases [50].

The formation of porosity in the compound layer can be explained by various mechanisms proposed over time. This being identified not only in ε-phase nitrides but also in other Fe-N phases such as γ' nitride [53-55]. Prenosil was the first to assume that porosity is a consequence of the appearance of N_2 molecular nitrogen within the layer [53].

Pore development requires desorption of nitrogen molecules. This will not occur in Fe-N phases at temperatures below 460 ˚C, it develops in the region of highest nitrogen content [50]. In an attempt to improve the performance of nitrided coatings, for example corrosion performance, various post-nitriding treatments have been undertaken.

2.4 Methods of kinetic growth

Gaseous nitriding is a thermochemical process that can be slow and expensive. There are various methods of accelerating the kinetics of nitriding, among which can be listed:

- the use of specific gas mixtures used in nitriding, adjusted to accelerate the kinetics of the process. For example, adding hydrogen to the nitrogen mixture can increase the diffusion rate of nitrogen atoms and reduce the time required for nitriding.
- the application of magnetic or electric fields can increase the mobility of nitrogen ions and accelerate their diffusion into the material to be nitrided. This method is known as magnetic or electric field assisted nitriding.
- using high temperatures, heating the material to higher temperatures than those normally used can accelerate the diffusion of nitrogen atoms.
- fluidized bed nitriding [66].

- oxynitriding.
- use of low pressures (vacuum) [67], or high pressures [68].

CHAPTER 2 - EXPERIMENTAL PART

4.1.1 Influence of the degree of ammonia dissociation on the kinetics of nitride layer growth

In order to understand the main parameters influencing the growth kinetics of the layers, a second-order non-compositional program was carried out (Table 4.1). With this methods which analysed the layers obtained on FeArmco and 34CrAlMo5 steel matrices under certain strict processing conditions where temperature and degree of dissociation were varied. The temperature varies in the range 540 ˚C - 620 ˚C and the degree of ammonia dissociation varied in the range 45% - 70%. The corresponding layer sizes for the two materials studied are given in Tab. 4.1.

Tabel 4.1. The central compositional orthogonal programming matrix of second order, K=2; actual conditions for carrying out the experiments and the results obtained [125]

Factor	Xo	**Independend variables (Xi)**							**Ytot,µm**	
									Fe-ARMCO	**34CrAlMo5**
		X_1	X_2	X_1X_2	X_1^2	X_2^2	X_1’	X_2’	**N**	**N**
Basic level	-	Z_0=580	Z_0=57,5	-	-	-	-	-	-	-
Variation Range	-	ΔZ=40	ΔZ=12,5	-	-	-	-	-	-	-
Higher level	-	Z_0+ΔZ= 620	Z_0+ΔZ=70	-	-	-	-	-	-	-
Lower level	-	Z_0-ΔZ= 540	Z_0-ΔZ=45	-	-	-	-	-	-	-
1	+1	-1	-1	+1	+1	+1	+1/3	+1/3	**484**	**200**
2	+1	-1	+1	-1	+1	+1	+1/3	+1/3	**477**	**160**
3	+1	+1	+1	+1	+1	+1	+1/3	+1/3	**1007**	**302**
4	+1	+1	-1	-1	+1	+1	+1/3	+1/3	**1224**	**313**
5	+1	+1	0	0	+1	0	+1/3	-2/3	**1113**	**309**
6	+1	-1	0	0	+1	0	+1/3	-2/3	**479**	**180**
7	+1	0	+1	0	0	+1	-2/3	+1/3	**682**	**172**
8	+1	0	-1	0	0	+1	-2/3	+1/3	**696**	**213**
9	+1	0	0	0	0	0	-2/3	-2/3	**685**	**201**

After statistical verification of the model coefficients, the particular shapes encoded for the two materials studied are obtained:

The particular form of the regression equation for FeArmco is:

$$Y=\delta tot=687,7+317,3X_1-39,6X_2-52,5X_1X_2+109,6X_1^2 \quad [125] \qquad (32)$$

The particular form of the regression equation for 34CrAlMo5 is:

$$Y=\delta tot=194,3+64X_1-15,3X_2+7,25X_1X_2+50,6X_1^2 \quad [125] \qquad (33)$$

In Fig. 4.1. and Fig. 4.2. the dependences obtained for pure technical iron and nitralloy steel, nitriding in a ammonia dissociated atmosphere at various temperatures and degrees of dissociation for an isothermal holding time of 4 hours are plotted. The results used for plotting dependencies were obtained by calculating regression equations.Analysing the two particular regression equations for the studied materials, it is observed that an increase in temperature (X_1) influences the size of δ1, much more strongly in the case of FeArmco compared to 34CrAlMo5 (317.5 µm compared to 64 µm). On the contrary, an increase in the degree of dissociation (X_2) relative to the base value chosen in the model leads to a decrease in the layer size. The simultaneous variation of the two parameters (X_1X_2) within the variation limits imposed by the model in the case of Fe-Armco is found to lead to a slight decrease in the total layer size, in contrast to the case of nitralloy steel, where a slight increase in the layer size is observed. Observing the value of X_1^2 it is much higher in the case of Fe-Armco than in the case of nitralloy steel, thus the effect of the component, which compensates this decrease. Overall, the simultaneous variation of these is also positive, beneficial in terms of total layer size. The type of programming adopted is correct and expresses with maximum probability the link between the variables and independent variables.

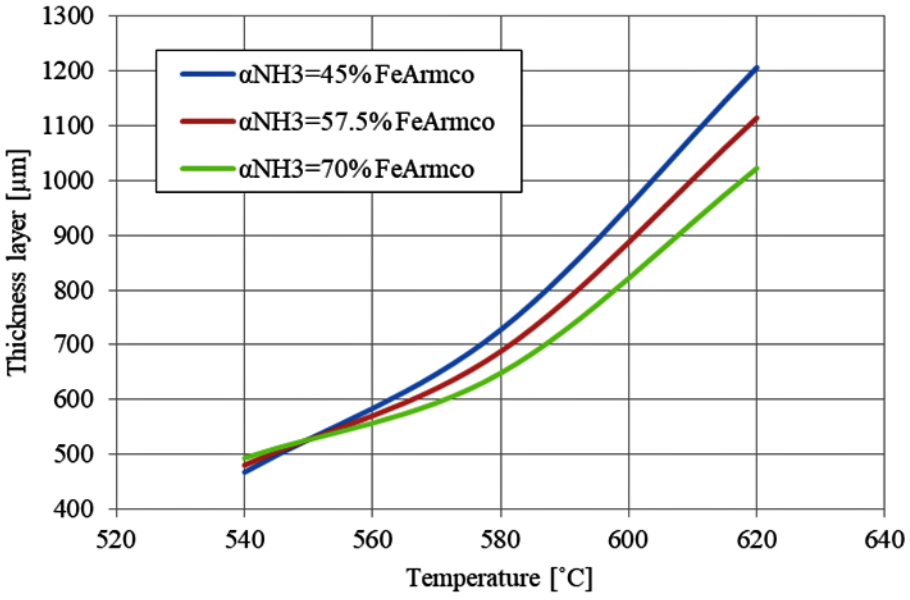

Figure 4.1. Variation curves of layer thickness versus temperature and degree of dissociation for Fe-Armco, nitrided in dissociated ammonia atmosphere, holding time 4 h.

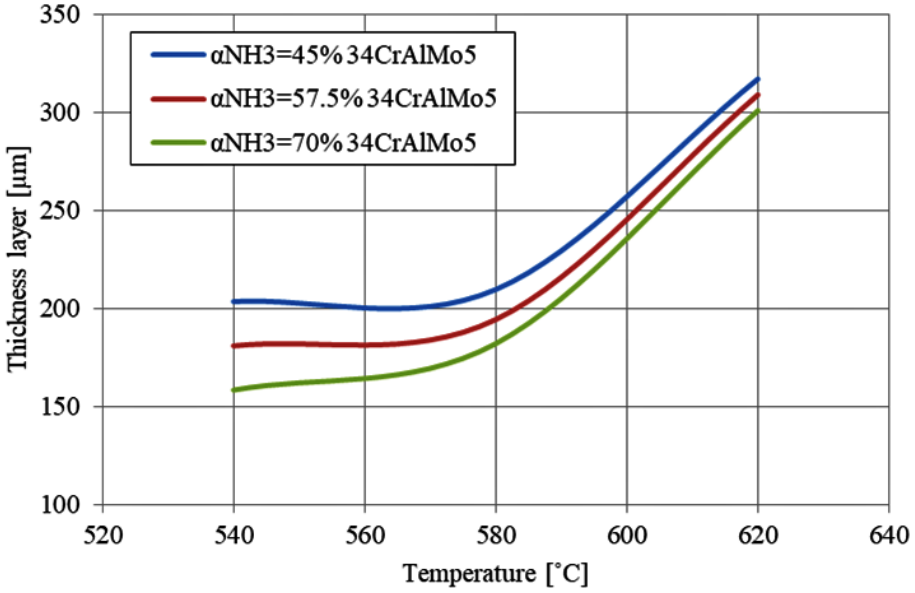

Figure 4.2. Variation curves of layer thickness as a function of temperature and degree of dissociation for 34CrAlMo5, nitrided in dissociated ammonia atmosphere, holding time 4 h.

The most intense kinetics is recorded for the 70% degree of dissociation, followed by 57.5% and the last 45%. However at 620 ˚C temperature and 45% dissociation degree, both Fe-Armco and 34CrAlMo5 obtained the highest layer values. Comparing the two figures (Fig. 4.1. and Fig. 4.2.), we observe the importance of the degree of dissociation in the temperature range 540-580 ˚C. Of greater importance in the kinetics of layer growth is the temperature, with the rate of reaction being strongly influenced by it. The degree of dissociation does not have a strong effect on the layer growth kinetics, but it has been observed that the value of 45% can be considered optimal, increasing the value above this leads to a decrease in the layer growth kinetics [125].

4.1.2 Modification of atmospheric activity by dilution of ammonia atmosphere with nitrogen

The non-compositional second-order programming method with K=3 had a total of 15 experiments (Table 4.6.)

.Tabel 4.6. The central necompositional programming matrix of second order, K=3; actual conditions for carrying out the experiments and the results obtained [106]

Factor	Temperature, ^{o}C		D,%		Proportion of nitrogen in the mixture,%		Total nitrided layer size,**Y**,µm	
	Natural values ^{o}C,Z_1	Coded values X_1	Natural values ^{o}C, Z_2	Coded values X_2	Natural values, ^{o}C,Z_3	Coded values X_3	**Fe-ARMCO**	**34CrAlMo5**
Basic level	Zo=580	0	Zo=45	0	Zo=30	0	-	-
Variation	ΔZ=40	-	ΔZ=25	-	ΔZ=30	-	-	-

range								
Higher level	Zo+ΔZ= 620	+1	Zo+ΔZ= 70	+1	Zo+ΔZ =60	+1	**-**	**-**
Lower level	Zo-ΔZ =540	-1	Zo-ΔZ =20	-1	Zo-ΔZ =0	-1	**-**	**-**
Exp.1	620	+1	70	+1	30	0	**991,9**	***253,3***
Exp.2	620	+1	20	-1	30	0	**954,7**	***238,04***
Exp.3	540	-1	70	+1	30	0	**561,4**	***191,12***
Exp.4	540	-1	20	-1	30	0	**573,6**	***170,76***
Exp.5	620	+1	45	0	60	+1	**1026,3**	***280,1***
Exp.6	620	+1	45	0	0	-1	**1224**	***313***
Exp.7	540	-1	45	0	60	+1	**670,9**	***166,34***
Exp.8	540	-1	45	0	0	-1	**479**	***180***
Exp.9	580	0	70	+1	60	+1	**790,2**	***138,86***
Exp.10	580	0	70	+1	0	-1	**682**	***172***
Exp.11	580	0	20	-1	60	+1	**799,9**	***176,93***
Exp.12	580	0	20	-1	0	-1	**696**	***213***
Exp.13	580	0	45	0	30	0	**768,9**	***175,53***
Exp.14	580	0	45	0	30	0	**720**	***190***
Exp.15	580	0	45	0	30	0	**813**	***167***

In order to highlight the importance of the nitriding atmosphere and how it influences the kinetics of layer growth as well as the phase composition of the layers, the nitriding atmosphere formed from dissociated ammonia was diluted with nitrogen.

After statistical verification of the model coefficients, the particular shapes encoded for the two materials studied result:

Regression equation for Fe-Armco:

$$\mathbf{Y=\delta_{tot}=767,3+226,5X_1-97,4X_1X_3+92,8X_1^2-85,8X_3^2} \quad [106] \qquad (35)$$

Regression equation for 34CrAlMo5:

$$\mathbf{Y=\delta_{tot}=177,5+47,02X1-14,47X3+47,75X_1^2} \quad [106] \qquad (36)$$

Analysing the particular regression equations for the studied materials, it is again observed that an increase in temperature (X_1) strongly influences the layer size in the sense of layer growth, much more intensely in the case of Fe-Armco compared to 34CrAlMo5 (226.5 µm compared to 47.02 µm). In the case of FeArmco, the degree of ammonia dissociation as a singular factor has no statistically significant influence. In the chosen range of variation, in the case of nitrogen dilution, the variation of the degree of dissociation does not statistically significantly influence the layer size.

By processing the particular regression equations for Fe-Armco, information on the influence of technological parameters can be obtained (Fig. 4.5.).

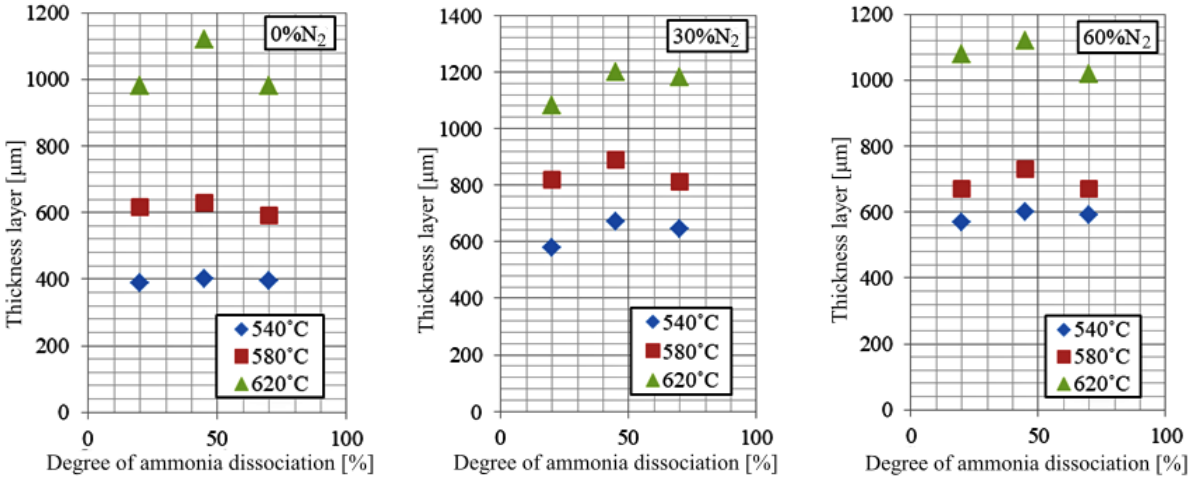

Figure 4.5. The influence of the technological parameters of gaseous nitriding; the degree of ammonia dissociation and the dilution with nitrogen of the gaseous atmosphere, αNH_3 = 20÷70%; 0 / 30 / 60 %N_2, on the total nitrided thickness layer, in the case of Fe-Armco, 4 h holding time.

Experimental studies show that a 30% N_2 dilution of the dissociated NH_3 atmosphere provides an enhancement of the overall kinetics of the layer to dissociation degree values around 45%. The 60% N_2 dilution of the atmosphere also shows an enhancement of the kinetics compared to a simple atmosphere consisting only of dissociated NH_3. Dilution of the atmosphere with 60% N_2 shows lower values compared to a 30% dilution of the atmosphere.

By working out the particular regression equations for nitralloy steel, information on the influence of technological parameters is obtained (Fig. 4.6.).

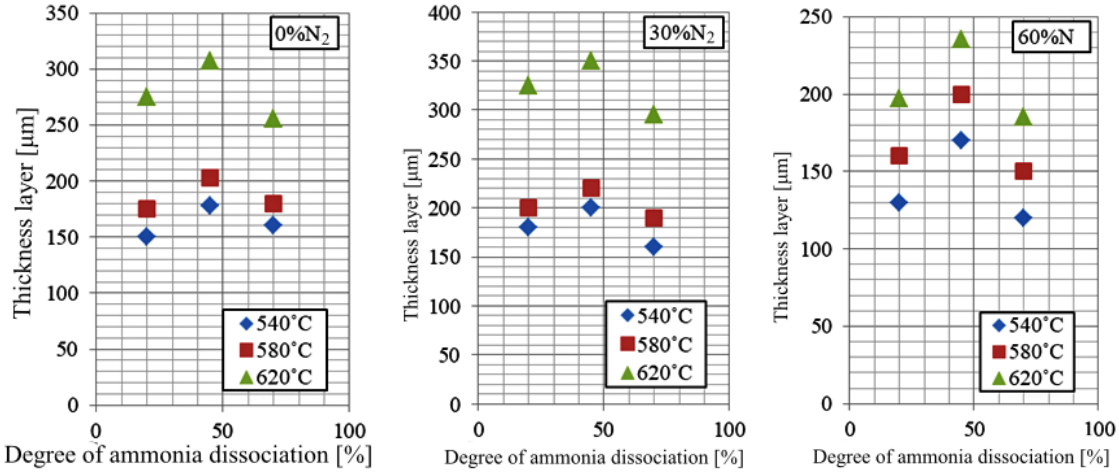

Figura 4.6. The influence of the technological parameters of gaseous nitriding; the degree of ammonia dissociation and the nitrogen dilution of the gaseous atmosphere, αNH_3 = 20÷70%; 0 / 30 / 60 %N_2, on the total nitrided thickness layer, in the case of 34CrAlMo5 steel, 4 h holding time.

It has been demonstrated and experimentally confirmed that the degree of ammonia dissociation from the ammonia-nitrogen gas mixture, together with the degree of nitrogen dilution of the medium, significantly influences the nitrogen potential of the gas mixture used for nitriding and thus the equilibrium nitrogen concentration at the thermochemically

processed metal-medium interface. If the proportion of nitrogen in the NH_3-N_2 mixture increases (within the limits of the mathematical model adopted), the nitrogen potential of the atmosphere increases, the more intensely the degree of dissociation of ammonia is reduced (towards the lower limit of the model adopted), thus implying an amplification of the growth kinetics of the nitrided layer.

The advantages of the nitrogen dilution are related not only to the acceleration of the layer growth kinetics but also to the considerable reduction of the brittleness of the surface area of the formed layers.

4.1.3 Predictions of the phasic composition of nitrided layers upon changes in the activity of the media used (undiluted ammonia atmospheric nitriding)

In order to control the phase composition of the nitriding layer, it is necessary to determine the correlation between the nitrogen potential of the atmosphere used (undiluted ammonia) and its degree of dissociation at the processing temperature. Achieving this desideratum is possible by rigorously correlating the information obtained from the explanation of the dependence between the degree of ammonia dissociation αNH_3, the nitrogen potential of the atmosphere π_N and the overpressure in the thermal aggregate workspace (p=1.012 atm), i.e. the demarcation limits of the $\alpha_N \leftrightarrow \gamma'$ and $\gamma' \leftrightarrow \varepsilon$ domains. This can be determined using the following equation:

$$\pi_N = \frac{(1-\alpha)(1+\alpha)^{0,5}}{(1{,}5\cdot\alpha)^{1,5}} \cdot p_t^{-0,5} \quad (129) \qquad (38)$$

where:

π_N - is the nitrogen potential;

P_t - is the pressure in the workspace.

$$\lg \pi_N^{\alpha\leftrightarrow\gamma'} = \frac{1120}{T} - 2{,}1 \text{ [129]} \qquad (39)$$

$$\lg \pi_N^{\gamma'\leftrightarrow\varepsilon} = \frac{1900}{T} - 2{,}3 \quad \text{[129]} \qquad (40)$$

Variation of the degree of dissociation for an atmosphere formed from undiluted ammonia in the range αNH_3=10 - 90% at 520 ˚C results in a change of nitrogen potential from 16.17 atm-0.5 to 0.087 atm-0.5 , as shown in Fig. 4.11. [130].

Thus, if it is desired to obtain a layer composed exclusively of nitroferrite, at 520 ˚C, the degree of dissociation of ammonia must be 80%, thus ensuring a nitrogen potential of the medium of maximum 0.2029 and thus a maximum concentration of nitrogen in the surface of the solid solution of 0.07227 %.

If the nitride layer is desired to have a $\gamma' > \alpha_N > \alpha$ phase zone, the nitrogen potential must be modified in accordance with the requirement, which is possible by varying the degree of ammonia dissociation.

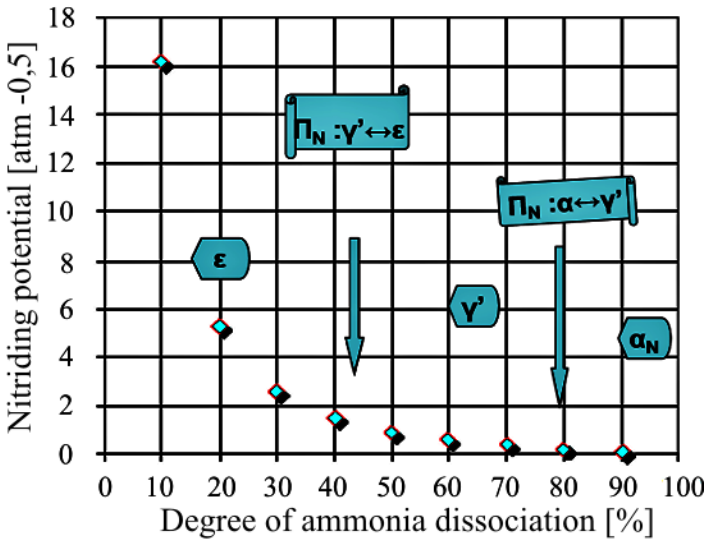

Figure 4.11. Variation of the nitrogen potential of the undiluted ammonia atmosphere depending on the degree of ammonia dissociation. [130]

Thus, as demonstrated above, at 520 ˚C, this requirement is achievable by providing a degree of dissociation of 60% and thus a nitrogen potential of 0.59 atm -0.5.

If is desired to obtain a solid solution zone based on the $Fe_{2-3}N$ compound, i.e. a layered phase sequence $\varepsilon > \gamma' > \alpha_N > \alpha$, the degree of dissociation of ammonia must be at most 30% at a temperature of 520 ˚C in order to ensure a nitrogen potential of at least 2.628 required to stabilise this phase at the surface.

From the comparative analysis of the evolution in time of the size of the three component phases of the nitrided layer, it is observed that the growth kinetics of the gamma prime phase is the slowest, an aspect related to the high degree of stoichiometry of this phase, it is followed by the epsilon phase in which the calculated variation of the nitrogen concentration at the temperature in question (520 ˚C) is between the limits 7.739 and 7.905%, followed by nitroferrite.

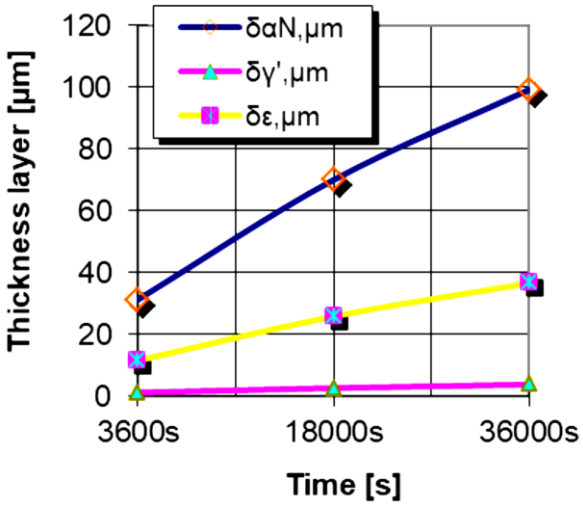

Figure 4.16. Comparative analysis of the growth kinetics over time, at temperature-520 ˚C, of the structural components of the nitrided layer obtained in the case of pure iron. .[130]

4.2 Modification of the growth kinetics of nitriding layers in the presence of surface layers with different chemical and phase composition than the original metal matrix (cemented with titanium and aluminium before nitriding)

In order to observe the effects of the growth kinetics of nitrided layers in the presence of surface layers, a thermochemical enrichment treatment of the materials used (Fe-Armco and 34CrAlMo5) with Ti and Al prior to nitriding was adopted (the sample titanliting are note TA).

The layers obtained from the thermochemical titanaliting processing for Fe-Armco (Fig. 4.17.-a)) and for 34CrAlMo5 steel (Fig. 4.17.-b)) can be seen below. In both cases, the zone enriched in titanium and aluminium compounds is well defined.

Using a central compositional second-order experimental program for K=2, varying temperature and the degree of dissociation, helps to understand the influence that enrichment with these subsequent elements has on nitriding kinetics. In Tab. 4.11. is describes the experimental program adopted to obtain this information.

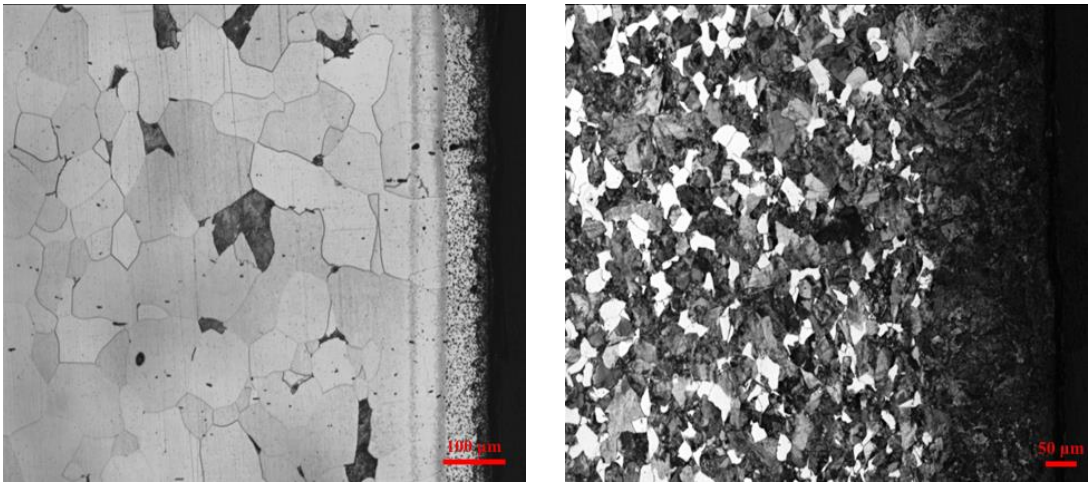

a) b)

Figura 4.17. Optical microscopy of (a) Fe-ARMCO and (b) 34CrAlMo5 after titanaliting in solid medium powder at 1050 oC/2 hours; Attacked reagent: nital 3%. [126]

Tabel 4.11. The central compositional orthogonal programming matrix of second order K=2; actual conditions for carrying out the experiments and the results obtained; Results of obtained layer for the materials used, titanaliting and subsequent nitriding [125]

Factor	Xo	Independent variables (Xi)							Y_{tot}, [µm]	
									FeArmco	34CrAlMo5
		X_1	X_2	X_1X_2	X_1^2	X_2^2	X_1'	X_2'	TA+N	TA+N
Basic level	-	Z_0=580	Z_0=57,5	-	-	-	-	-	-	-
Variation range	-	ΔZ=40	ΔZ=12,5	-	-	-	-	-	-	-
Higher level	-	Z_0+ΔZ=620	Z_0+ΔZ=70	-	-	-	-	-	-	-

Lower level	-	Z_0-ΔZ=540	Z_0-ΔZ=45	-	-	-	-	-	-	-
1	+1	-1	-1	+1	+1	+1	+1/3	+1/3	***383***	**178**
2	+1	-1	+1	-1	+1	+1	+1/3	+1/3	***396***	**146**
3	+1	+1	+1	+1	+1	+1	+1/3	+1/3	***954***	**272**
4	+1	+1	-1	-1	+1	+1	+1/3	+1/3	***1150***	**307**
5	+1	+1	0	0	+1	0	+1/3	-2/3	***1053***	**291**
6	+1	-1	0	0	+1	0	+1/3	-2/3	***390***	**165**
7	+1	0	+1	0	0	+1	-2/3	+1/3	***587***	**180**
8	+1	0	-1	0	0	+1	-2/3	+1/3	***645***	**190**
9	+1	0	0	0	0	0	-2/3	-2/3	***613***	**179**

After statistical verification of the model coefficients the particular shapes encoded for the two studied materials result:

The particular form of the regression equation for Fe-Armco TA + N:

$$\mathbf{Y=\delta tot=615,6+331,3X_1-40,1X_2-52,2X_1X_2+106X_1^2} \quad [125] \qquad (53)$$

The particular form of the regression equation for 34CrAlMo5 TA + N:

$$\mathbf{Y=\delta tot=176,5+63,5X_1-15,6X_2+50,9X_1^2} \quad [125] \qquad (54)$$

Analyzing the particular regression equations for the two studied materials, it is observed also in this case that an increase in temperature (X_1) influences the size of δ, much more strongly in the case of Fe-Armco compared to 34CrAlMo5 (615.5 μm compared to 194.3 μm). An increase in the degree of dissociation (X_2) relative to the base value chosen in the model leads to a decrease in the layer size. The simultaneous variation of the two parameters (X_1X_2) within the limits imposed by the model, in the case of Fe-Armco is observed to cause a slight decrease in the total layer size, unlike in the case of 34CrAlMo5 steel where a slight increase in the layer size is observed (-52.2 compared to +7.25). Analysing the value of X_1^2 it is much higher for pure iron than for nitralloy steel, thus the effect of the non-linear component appears, which compensates this decrease. Overall the simultaneous variation of these is also positive, beneficial in terms of total layer size.

The type of programming adopted is correct and expresses with maximum probability the relationship between dependent and independent variables.

By processing the particular regression equations it is possible to obtain information on the influence of the technological parameters, thus with their help the curves of variation of the degree of dissociation as a function of temperature were obtained (Fig. 4.18.).

From the dependencies present in Fig. 4.18. and Fig. 4.19., the importance of temperature increase on the overall growth kinetics of the layers can be seen. Comparing the

titanaliting and then the simple nitrided layers with the plain nitrided layers, a slight decrease in the total thickness of the titanaliting and nitrided layers can be observed.

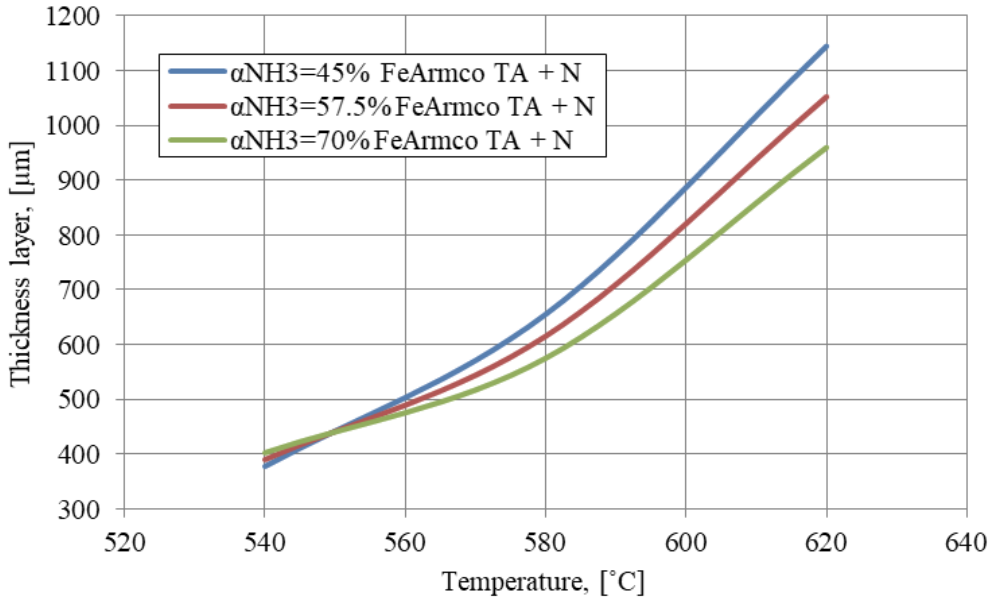

Figure 4.18. Variation curves of layer thickness as a function of temperature and degree of dissociation for Fe-Armco titanaliting at 1050 ˚C/2 h and nitrided in dissociated ammonia atmosphere at various degrees of dissociation (α=45%, α=57.5%, α=70%) holding time 4h.

Due to the existence of a rich zone of titanium and aluminium compounds that form nitrides during the process, the amount of available nitrogen is reduced. Increasing the degree of dissociation for both titanaliting and nitrided pure technical iron samples and titanaliting and nitrided 34CrAlMo5 steel has a negative effect on the overall layer formation kinetics.

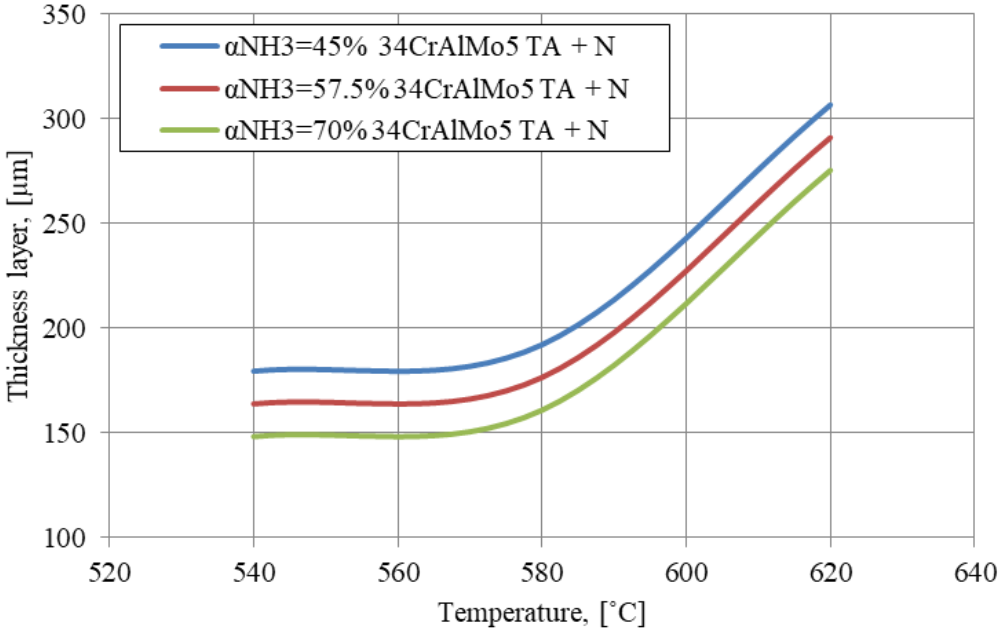

Figure 4.19. Variation curves of layer thickness as a function of temperature and degree of dissociation for 34CrAlMo5 titanaliting at 1050 ˚C/2 h and nitrided in dissociated ammonia atmosphere at various degrees of dissociation (α=45%, α=57.5%, α=70%) holding time 4.

With electron microscopy it was possible to characterize the titanaliting layers and then the titanaliting and nitrided layers. Thus in Fig. 4.24 and Fig. 4.25 are show the layer structures for the studied materials (Fe-Armco and 34CrAlMo5).

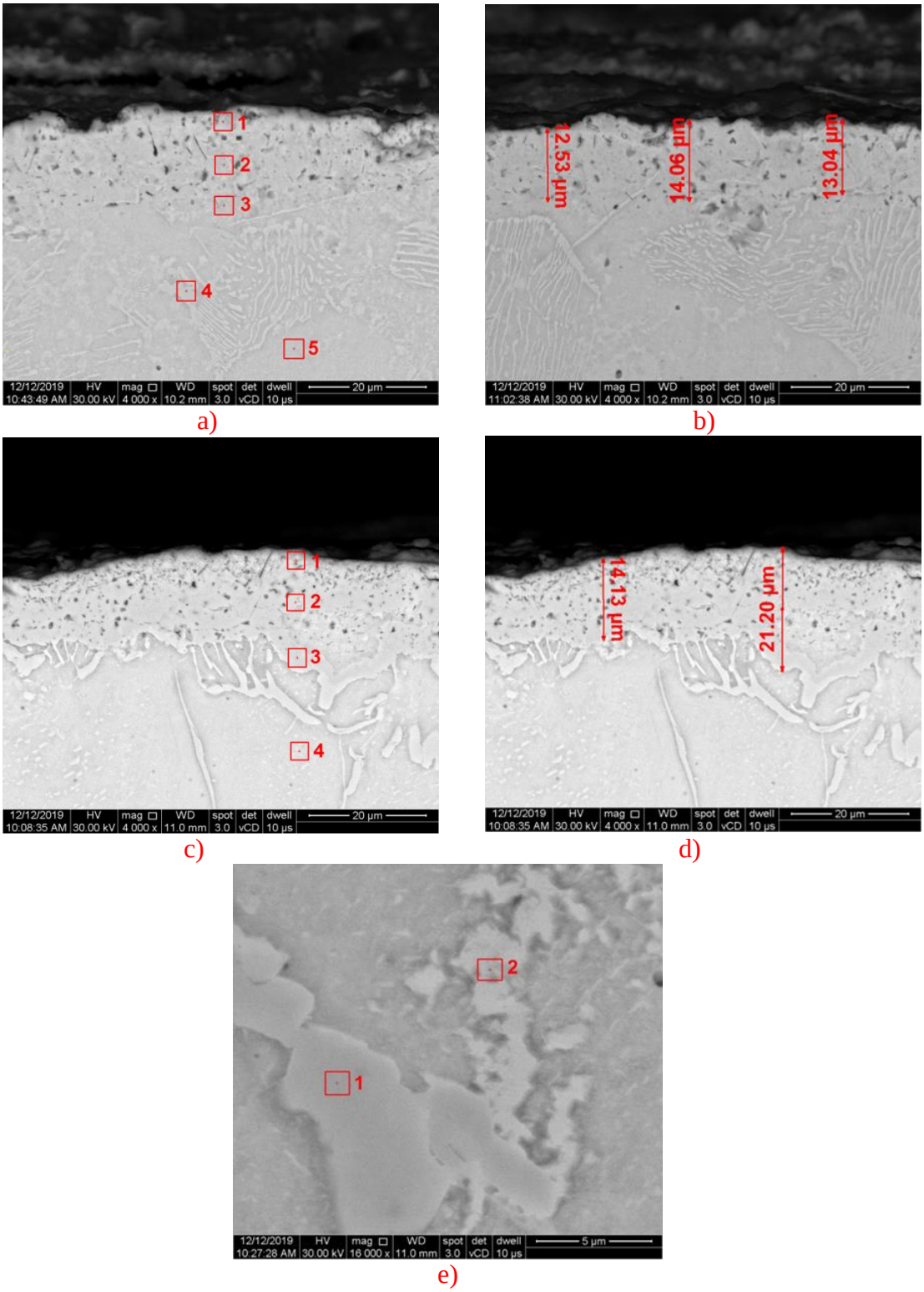

Figura 4.24. Electronic microscopy for : a) Fe-Armco titanaliting at 1050 ˚C / 2 hours; b) Fe-Armco titanaliting at 1050 ˚C / 2 hours-thick layer; c) Fe-Armco titanaliting and nitrided at 580 ˚C / 4 hours with αNH_3=45%; d) Fe-Armco titanaliting and nitrided at 580 ˚C / 4 hours with αNH_3=45% layer thickness; e) Fe-Armco titanaliting and nitrided at 580 ˚C / 4 hours with αNH_3=45% diffusion zone analysis points.

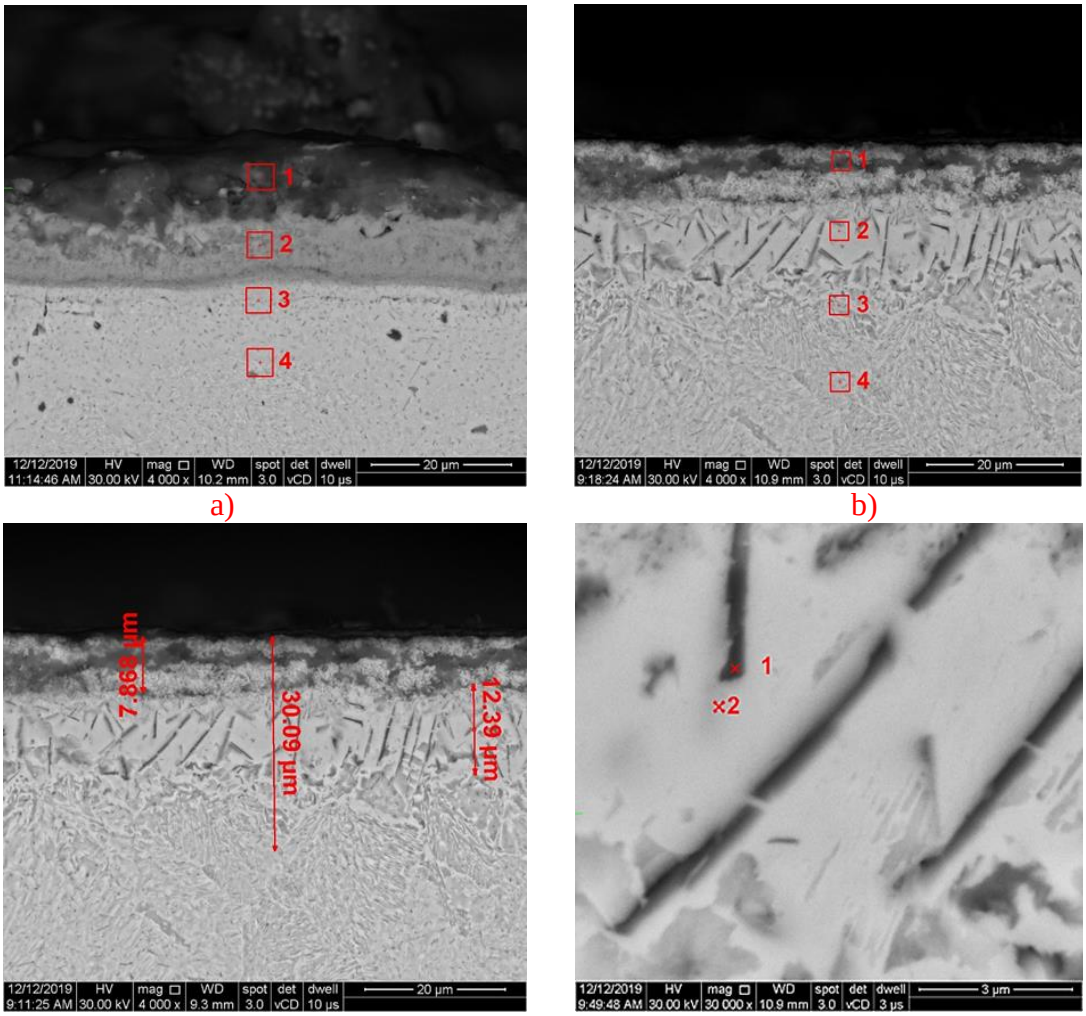

Figura 4.25. Electronic microscopy for : a) 34CrAlMo5 titanaliting at 1050 ˚C / 2 hours; b) 34CrAlMo5 titanaliting and nitrided at 580 ˚C / 4 hours with αNH_3=45%; c) 34CrAlMo5 titanaliting and nitrided at 580 ˚C / 4 hours with αNH_3=45% layer thickness; d) 34CrAlMo5 titanaliting and nitrided at 580 ˚C / 4 hours with αNH_3=45% analysis points for the phases in the layer.

Table 4.16. Chemical composition of elements found in microvolumes shown in Fig. 4.24-a) Fe-Armco titanaliting at 1050 ˚C / 2 hours

	C	O	F	Al	Ca	Ti	Fe
Zona 1	4,23	2,03	13,76	4,31	0,82	0,72	74,14
Zona 2	2,41	1,18	10,22	2,23	0,71	0,70	82,54
Zona 3	1,72	1,03	9,75	2,91	0,75	0,64	83,21
Zona 4	2,32	-	-	-	-	-	97,68
Zona 5	2,75	-	-	-	-	-	97,25

Table 4.20. Chemical composition of elements found in microvolumes shown in Fig. 4.25.-a) 34MoCrAl5 titanaliting at 1050 ˚C 2 h

	C	O	F	Mg	Al	Si	Ca	Ti	Cr	Fe	Mn
Zona 1	5,14	22,7	9,24	1,22	35,22	0,91	6,92	2,81	0,66	15,18	-
Zona 2	3,73	18,77	9,92	1,18	3,98	0,98	2,61	0,85	0,65	57,33	-
Zona 3	-	10,95	7,49	-	7,5	1,4	0,86	0,81	1,17	69,82	-

Zona 4	-	-	-	-	3,39	1,44	-	-	2,17	90,77	2,24
Z 5	-	-	-	-	2,96	1,42	-	-	2,16	91,47	1,98

X-ray diffraction for pure technical iron titanaliting and nitrided (Fig. 4.26) revealed the phases forming in the layers obtained. Thus iron nitrides, aluminium nitrides and titanium nitrides were found.

X-ray diffraction on 34CrAlMo5 steel (Fig. 4.27) reveals the phases that form in the titanaliting and subsequently nitrided layers. Nitrides of aluminium, titanium, iron, molybdenum but also iron titanides (Fe_2Ti) were observed.

All these compounds are present only in the surface areas of the layers. As shown by electron microscopy and chemical microanalysis.

The layer of aluminium-titanium compounds formed during thermochemical titanaliting processes does not constitute a barrier to nitrogen diffusion. Under certain conditions of temperature and degree of dissociation, the value of the layers obtained after nitriding is slightly increased.

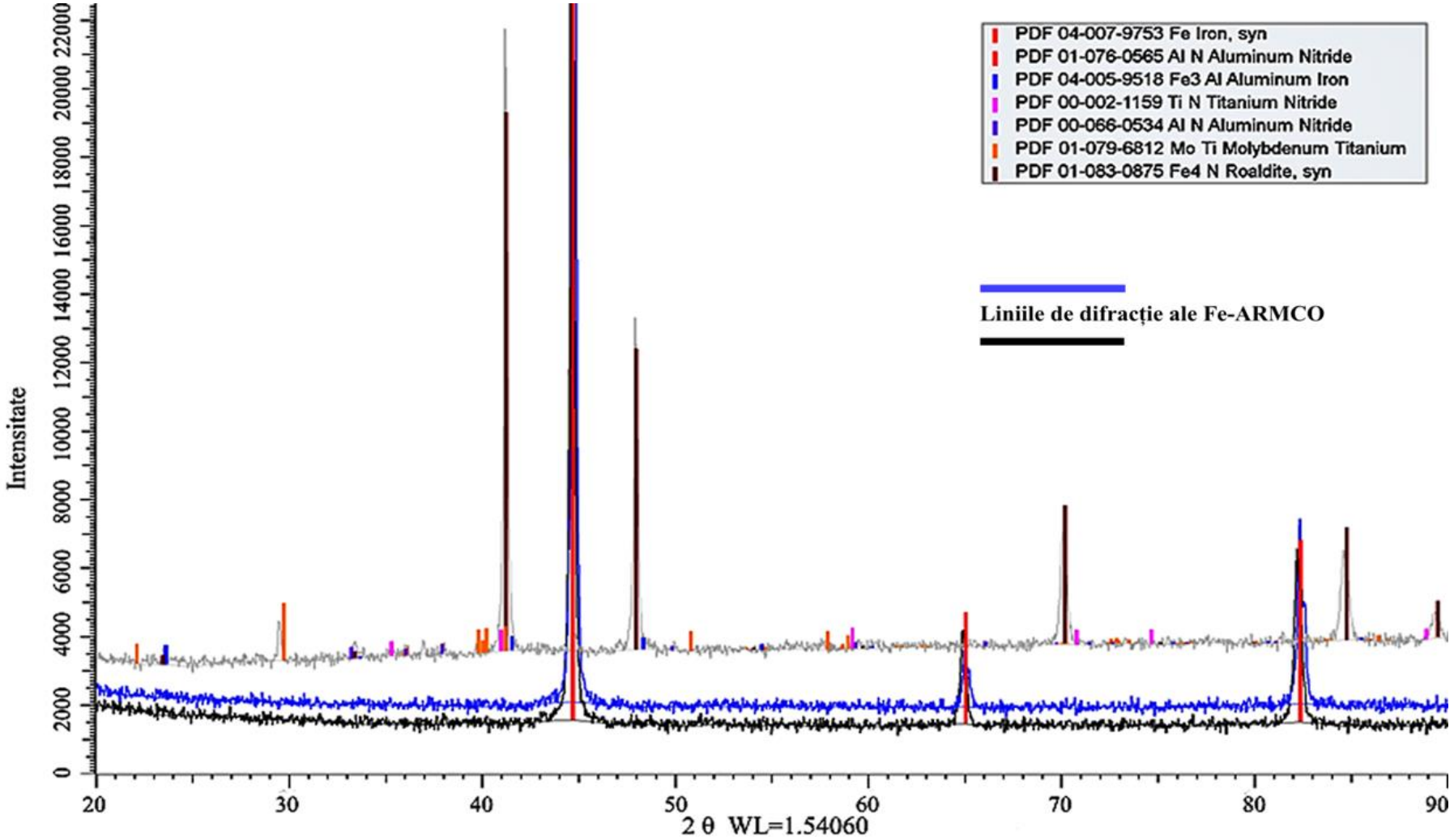

Fig. 4.26. X-ray diffraction of titanaliting technical pure iron in solid medium powder (1050 oC/2 hours) and subsequently nitriding in partially dissociated ammonia (580 oC / 4 hours; αNH_3 = 45%)
Note: The two basic lines represent the diffraction lines of technical pure iron (reference). [126]

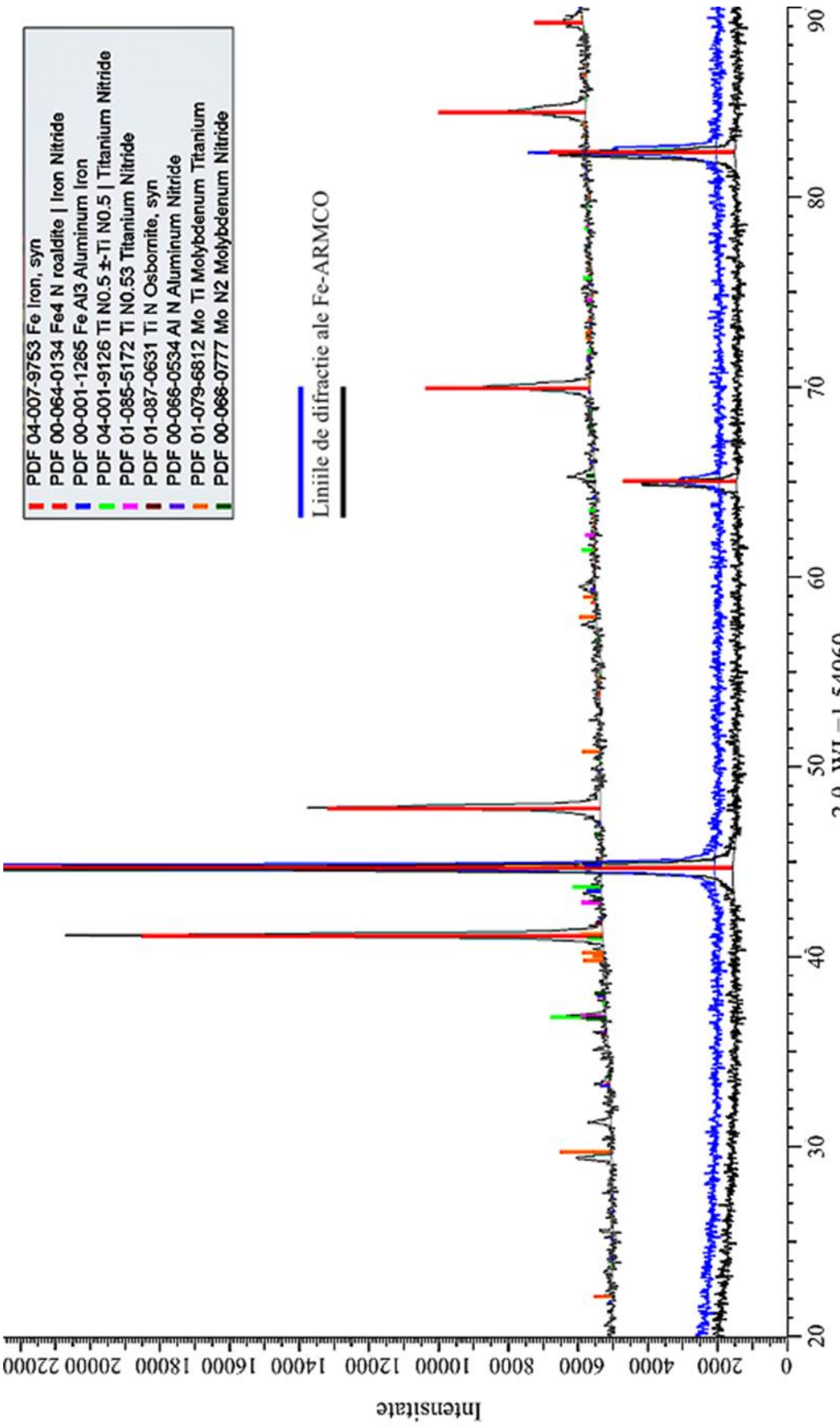

Fig. 4.27. X-ray diffraction of titanaliting 34CrAlMo5 steel in solid medium powder (1050 oC / 2 hours) and subsequently nitriding in partially dissociated ammonia (580 oC/4 hours; αNH_3 = 45%)
Note: The two basic lines represent the diffraction lines of technical pure iron (reference). [126]

4.3 Semi-empirical methods for estimating the growth kinetics of nitriding layers

The package of experimental results used for statistical processing was obtained under the following conditions: temperature (500÷580 ˚C) and holding time (4÷12 hours) at a constant degree of dissociation αNH_3=40%.

4.3.1 Kazeev method

The Kazeev method is based on the premise that in parallel with atomic diffusion in the metal matrix, other interaction phenomena occur. Starting from the assumption that the dependence of the increase of state on time at a given temperature is parabolic, thus the total layer size is 〖h=β·t〗 ^m , it follows that lgh/lgn ~m. Based on the experimental data concerning the nitriding of pure technical iron, the time dependences of the nitrided layer size at different temperatures were plotted (Fig. 4.31.).

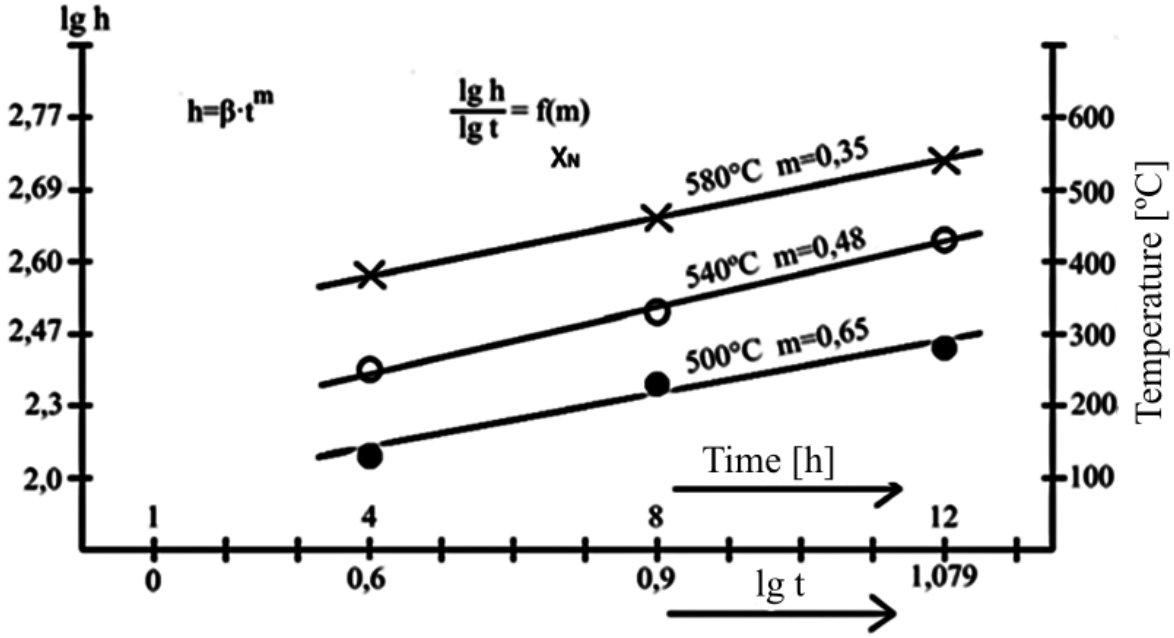

Figure 4.30. The anamorphosed dependence of the equation kinetics for the saturation by nitrogen diffusion of the pure technical iron. [136]

Statistical processing of the results concerning the two kinetic parameters, m and β (β=h/t^m), obtained by changing the process parameters (temperature and time), led to the following expressions of their temperature dependencies (Fig. 4.32):

$$m=2{,}518-0{,}00375\cdot T \quad [136] \tag{58}$$

$$\beta=-1{,}03+0{,}00216\cdot T \quad [136] \tag{59}$$

The evolution over time of the total layer size for pure technical iron at different temperatures can be described with the following equation:

$$h_{[mm]} = (-1{,}03 + 0{,}00216 \cdot T) \cdot t^{(2{,}518-0{,}00375\cdot T)} \quad [136] \tag{60}$$

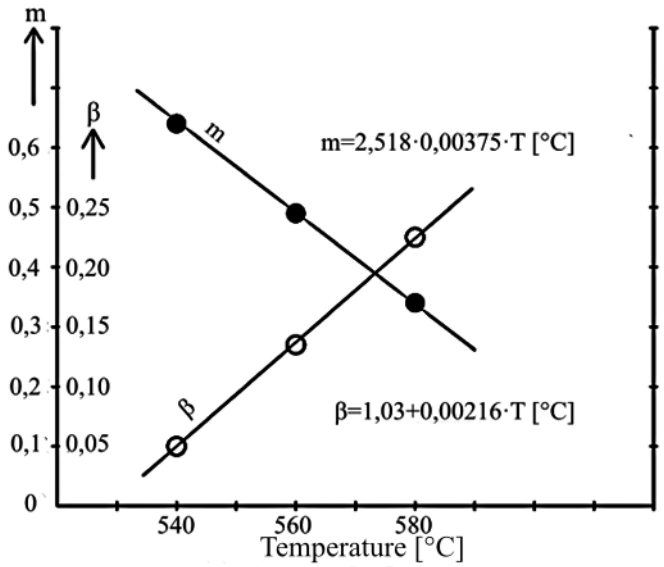

Figure 4.32. Dependence of kinetic parameter, β and m, by temperature. [137]

4.3.2 Baram method

The Baram method approaches the kinetics of thermochemical processing from the perspective of heterogeneous chemical reactions. It appeals to the law of mass action and the phenomenological dependence of the change in time of the positions of the interface separation surfaces (eq.65)

$$K^* = \frac{(1-\propto)V^n}{S_0 \cdot t^{1-\alpha}} \int_{m0}^{m} \frac{dm}{[CV-(m-m_0)]^n} \quad [123] \tag{65}$$

Translating the experimentally obtained information into logarithmic coordinates leads to the drawing of dependencies that provide information about the value of the kinetic component (Fig. 4.33.).

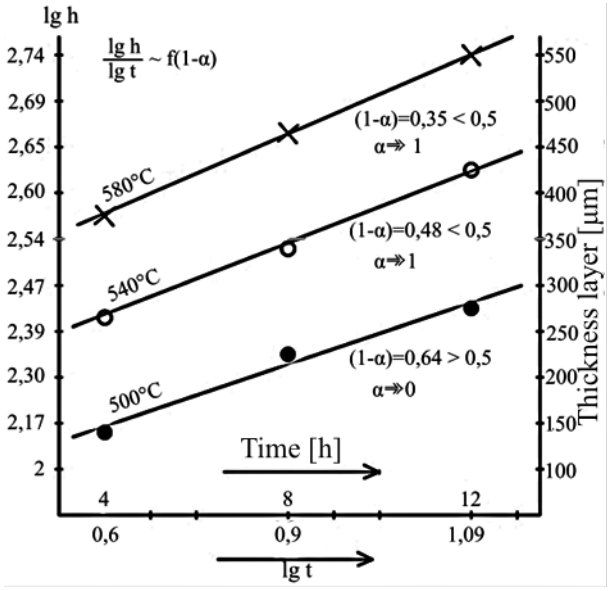

Figure 4.33. The anamorphosed dependence of equation kinetics, for saturation by nitrogen diffusion of the pure technical iron. [136]

With the help of the reaction constants K_0, it is possible to calculate the values of the total size of the nitrided layer as well as its growth rate using following equations:

$$h_{calc} = \frac{\overline{K_0}}{1-\alpha} \cdot t^{1-\alpha} \quad [123] \tag{68}$$

$$V = \frac{\overline{K_0}}{1-\alpha} \cdot t^{-\alpha} \quad [123] \tag{69}$$

4.3.3 Popov method

The graphical results according to the Popov method, which starts from the graphical expressions of the solutions of the differential equation solved analytically and criterially under third-order boundary conditions, are shown in Fig. 4.34. A particular approach in the model proposed is the knowledge of the moment at which the curves describing the evolution in time at different temperatures of the layer size, separate from the abscisa (Fig. 4.34).

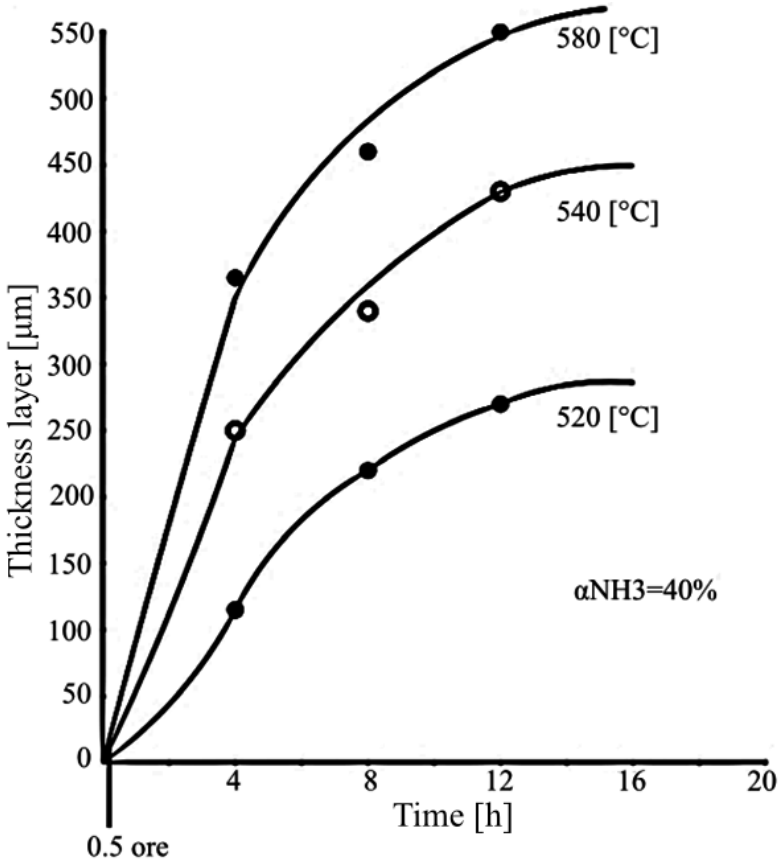

Figure 4.34. Dependence of all nitriding layer pbtained in the case of iron technically pure, by nitriding parameters. After 30 minutes, the layer becomes observable metallographically. [136]

The algorithm used to solve is as follows:

- Determine the relative concentration Θ

$$\Theta = \frac{C_{lim} - C_0}{C_{max} - C_0} \quad [124, 44] \tag{70}$$

- Calculate the Tihonov criterion:

$$Ti_1 = Ti_x \sqrt{\frac{t1}{tx}} \quad [124] \tag{71}$$

- The diffusion coefficient D is calculated using the Tikhonov criterion

$$D = (\frac{Ti}{h'})^2 \frac{1}{3600 \cdot t_1} [cm^2/s] \quad [124] \qquad (72)$$

- Calculate the adsorption rate constant K$K = h' \cdot D$ [124]
  (73)
- Estimate the layer size (h) using information related to the antecalculated diffusion coefficients $h = a\sqrt{D \cdot t}$ [124]
  (74)

Comparing the results obtained by the three methods for pure technical iron nitrided at various temperatures (500, 540 and 580 ˚C) in an ammonia atmosphere with a degree of dissociation αNH_3=40% with the results obtained experimentally, a very high degree of agreement is observed.

C2. PERSONAL AND ORIGINAL CONTRIBUTIONS

- An ammonia inlet pipe has been designed which is constructed in the form of a torus with differently oriented holes, thus achieving gas uniformity in the enclosure and at the same time better gas circulation.
- Experimental programing methods - the active experiment method - were used in each stage of the experimental investigations carried out on nitralloy - 34CrAlMo5 type steel and in parallel on Fe-Armco matrices; in this way it was possible to quantify the following with the help of regression equations: (i) the effects of changing the degree of ammonia dissociation on the kinetics of nitrided layer growth for the case where nitriding is a single thermochemical treatment or is applied after another thermochemical processing, i.e. titanaliting; (ii) the combined effect of the degree of dissociation and the degree of nitrogen dilution (in the case of atmospheres formed from ammonia diluted with nitrogen) on the kinetics of nitrided layer growth.
- It has been proposed that if a thermochemical cementate treatment with titanium and aluminium is applied prior to nitriding, the subsequent high-tempering treatment after volume martensitic hardening (in order to ensure an improving structure of the matrix to be nitrided and thus ensure the desired level of toughness) should be replaced by nitriding itself; in this way, in addition to the decomposition of the martensite, a considerable shortening of the total thermochemical processing cycle is ensured.
- Thermodynamic calculations were used to determine the correlation between the degree of ammonia dissociation and the nitrogen potential of the atmosphere, or concurrently the degree of ammonia dissociation - and the degree of nitrogen dilution

of the NH_3-N_2 atmosphere to estimate the change in the nitrogen potential of the atmosphere.

- The semi-empirical Kazeev-Baram and Popov methods were adapted to the need for instruments with which the growth kinetics of nitrided layers could be predicted; it was concluded that the use of such methods requiring a minimum number of experimental results leads to results very close to the experimental ones (errors of maximum 8÷10%).

ANNEXES

A1. Dissemination of the results of the PhD thesis research

1- Mihai Ovidiu Cojocaru, Leontin Nicolae Druga, Andrei Mihai **Ghinea**, Semi-empirical methods for estimation/prediction of metal matrices behavior during thermochemical processing, Materials Today: Proceedings, 19, 2019, 979-990, WOS:000496428200011.

2- **Andrei Mihai Ghinea**, Mihai Ovidiu Cojocaru, Leontin Nicolae Druga, Effects of nitriding subsequent titanaliting of steels, The Annals of ,,Dunarea de Jos" University of Galati, Fascicle IX. Metallurgy and Materials Science, no.2, 2020, 34-44, https://doi.org/10.35219/mms.2020.2.07.

3- Cojocaru Mihai Ovidiu, Branzei Mihai**, Ghinea Andrei Mihai**, Cotrut Cosmin, Druga Leontin, Nitriding in ammonia-nitrogen gaseous mixtures, after the simultaneous saturation with Ti and Al, International Journal of Surface Science and Engineering (Q4) 2022, WOS:000781378200002.

4- **Mihai Andrei Ghinea**, Mihai Ovidiu Cojocaru, Mihai Branzei, Leontin Nicolae Druga, Predictions regarding the effects of nitriding applied to steels in the absence or presence of titanaliting, U.P.B. Sci.Bull., Series B (Q4), vol 82, 2020, WOS:000610101300028.

5- Mihai Ovidiu Cojocaru, Mihai Branzei, **Andrei Mihai Ghinea**, Leontin Nicolae Druga, The effects of modifying the activity of nitriding media by diluting ammonia with nitrogen, Materials (Q2), 2021, 14, WOS:000650631700001.

6- Mihai Ovidiu Cojocaru, Mihai Branzei, Ciuca Sorin, Bogdan Florea, **Andrei Mihai Ghinea**, Florentina Georgiana Calin, Analytical method for estimating nitriding effects, U.P.B. Sci.Bull., Series B (Q4), vol 3, 2023, WOS:001052966300011.

SELECTIVE BIBLIOGRAPHY

[1] George Vermesan, Elena Vermesan; Nitrurarea in gaz; Editura Sid 48, 1986.

[3] Steiner, T., Mittemeijer, E.J.; Alloying Element Nitride Development in ferritic Fe-based Materials Upon Nitriding: A review; Journal of Materials Engineering and Performance, 2016, vol 25, June, 2091-2102, DOI: 10.1007/s 11665-016-2048-x.

[4] Dhafer Wadee Al-Rekaby, Kostyk V., Kostyk K., Glotka A., Chechel M.; The choice of the optimal temperature and time parameters of gas nitriding of steel; Eastern-European Journal of Enterprise Technologies, 2016, 3/5 (81), June, ISSN 1729-3774.

[7] Fry A.; Stickstoff in Eissen, Stahl und Sonderstahl Einneues oberflachen hartung svenfahren, Stahl und Eisen, 1923, vol 40, nr4.
[8] Paranjpe V.G., Morris Cohen,.Bever M.B, and Floe C.F.; The iron-Nitrogen System; Transactions Aime, Journal of Metals, 1950, vol.188, pp.261-267.
[9] Grieveson P., Turkdogan E.T.; Kinetics of Nitrogen Solutions in Alpha and Delta Iron; Metallurgical and Materials Transaction A, 1964, vol 230, pp. 1604-1609.
[10] Mittemeijer E.J.; Nitriding of binary and ternary iron-based alloys; Woodhead publishing Series in Metals and Surface Engineering, 2015, No 62.
[16] Somers M.A.J. and Mittemeijer E.J.; Harterei-Tech, Mitt., 1992, vol47, 5-12.
[18] Bohmer S., Spies H.I., Berg H.I., Zimdars H.; Oxyhen probes for controlling nitriding and nitrocarburising atmospheres; Surface Engineering, 1994, vol.10, no.2, pp.129-135.
[19] Kooi Bart J., Somers Marcel A.J., Mittemeijer Eric J.; An evaluation of the Fe-N Phase Diagram Considering Long-Range Order of N Atomns in γ'-Fe_4N_{1-x} and ε-Fe_2N_{1-z}; Metallurgical and Materials Transactions A, 1996, Vol 27 A, April, pp.1063-1071.
[20] Jack K.H.; Results of further x-ray structural investigation of the iron-carbon and iron-nitrogen systems and of related interstitial alloys; Acta Crystallogr., 1950, 3, 392-393.
[21] Kardonina N.I., Yurovskikh A.S., and Kolpakov A.S.; Transformation in the Fe-N system; Metal Science and Heat Treatment, 2010, No.52, pp-457-467, translate from Metallovedanie I Termicheskaya Obrabotka Metallov, no.10, pp-5-15.
[25] Naim Syla, Fisnik Aliaj, Nazmi Hasi; Study of the compound layer of gas nitride 31CrMoV9 steel; The 4th Global Virtual Conference, May 2016, pp.206-210, doi:10.18638/gv.2016.4.1.776.
[27] Holger Gohring, Olga Fabrichnaya, Andreas Leineweber, Eric Jan Mittemeijer; Thermodynamics of the Fe-N and Fe-N-C Systems: The Fe-N and Fe-N-C Phase Diagrams Revisited; Metallurgical and Materials Transaction A, 2016, Volume 47A, December, DOI: 10.1007/s11661-016-3771-0.
[33] Grabke H.J; Conclusion on the mechanism of ammonia-synthesis from the kinetics of nitrogenation and denitrogenation of iron; Zeitschrift fur Physikalische Chemie Neue Folge, 1976, Bd.100, S.185-200.
[37] Grabke H.J.; Reaktionen von Ammoniak, Stickstoff und Wasserstoff an der Oberflache von Eisen; I. Zur Kinetik der Nitrierung von Eisen mit NH_3-H_2-Gemischen und der Denitrierung; Berichte der Bunsegellschaft, 1968, Bd.72, nr. 4, pp.533-541.
[41] Slycke, J.T., Mittemeijer, E.J, Somers, M.A.J.; Thermodynamics and kinetics of gas and gas-solid reactions; Thermochemical Surface Engineering of Steels, 2015.
[44] Hosmani S.S., Schacherl R.E. and Mittemeijer E.J.; Nitrogen absorption by Fe-1.04 at% Cr alloy:uptake of excess nitrogen; Journal of Materials Science, 2008, 43, 8, pp.2618-2624, doi:10.1007/s10853-008-2473-9.
[47] Cojocaru M., Ciuca I., Druga L., Cosmeleata G.; Empirical exposition of the adsorbtions ionic mechanism on gaseous nitriding; Electical processes in engineering and chemistry, original text published in Elektronnaya Obrabotka Materialov, 2008, No5, pp.63-68, ISSN 1068-3755.
[50] Somers M.A.J.; Cap 8-Development of the compound layer during nitriding and nitrocarburizing of iron and iron-carbon alloys; Termochemical Surface Engineering of steels, 2015, pp.341-372, doi:10.1533/9780857096524.3.341.
[51] Ratajski J., Tacikowski J., Somers M.AJ.; Development of compound layer of iron (Carbo)nitrides during nitriding of steel; Surface Engineering, 2003, vol 19, no.4, 285-291, doi:10.1179/026708403225007455.
[53] Prenosil B.; New Knowledge about the structure of layers carbonitrided in a gas atmosphere of about 600˚C; Harterei-Technische Mitteilungen, 1973, vol.28, 157-164, ISSN: 0017-6583.

[54] Hoffman R., Mittemeijer E.J. and Somers MAJ.; Verbindungsschichtnildung beim nitrieren und nitrocarburieren; Harterei-Technische Mitteilungen, 1996, vol.51/3, 162-169.
[55] Mittemeijer E.J., Rooijen M.Van, Wierszyllowski J., Rozendaal H.C.F. and Colijin P.F.; Tempering of iron-nitrogen martensite; International Journal of Materials Research, 1983, Vol. 74, 473-487.
[66] Haruman E., Sun Y., Malik H., Sutjipto A.G.E., Mridha S., Widi K.; Low temperature fluidized bed nitriding of austenitic stainless steel; Solid State Phenomena, 2006, Vol.118, pp.125-130.
[67] Maldzinski L., Przygonski Tomasz, Kreuzaler, D.T.; Controlled nitriding using a Zeroflow process; 70 th Annual Congress, ABM week, Rio de Janeiro, 2015, pp.1941-1946, ISSN 1516-392X
[68] Marius Holger Wetzel, Tina Trixy Rabending, Martin Friak, Monika Vsianska, Mojmir Sob, Andreai Leineweber; Phase stability on iron nitride Fe4N at high pressure-pressure dependent evolution of phase equlibria in the Fe-N system; Materials, 2021, vol. 14, 3963, doi:10.3390/ma14143963.
[106] Mihai Cojocaru, Mihai Branzei, **Andrei Mihai Ghinea**, Leontin Druga; The effects of modifying the activity of nitriding media by diluting ammonia with nitrogen; Materials, 2021, 7; 14(9):2432, PMID:34067157
[123] Baram I.I., Lahtin Iu.M., Kogan I.D.; Kinetica protessov himico-termiceskoi obrabotki melallov i spavov; Mitom, 2019, nr.2.
[124] Popov A.A.; Teoreticeskoe osnova himico-termiceskoi obrabotki stali; Sverdlovsk, 1962
[125] **Mihai Andrei Ghinea**, Mihai Ovidiu Cojocaru, Mihai Branzei, Leontin Nicolae Druga; Predictions regarding the effects of nitriding applied to steels in the absence or presence of titanaliting; U.P.B. Sci.Bull., Series B, 2020, vol 82.
[126] **Andrei Mihai Ghinea**, Mihai Ovidiu Cojocaru, Leontin Nicolae Druga; Effects of nitriding subsequent titanaliting of steels; The Annals of „Dunarea de Jos" University of Galati, Fascicle IX. Metallurgy and Materials Science, 2020, no.2, 34-44.
[136] Mihai Ovidiu Cojocaru, Leontin Nicolae Druga, **Andrei Mihai Ghinea**; Semi-empirical methods for estimation/prediction of metal matrices behavior during thermochemical processing; Materials Today: Proceedings, 2019; vol.19, pp. 979-990.
[137] Mittemeijer E.J., Somers M.A.; Kinetics of thermochemical surface treatments; Thermochemical Surface Engineering of Steels, 1-st Edition Woodhead Publishing, sept. 2014